สัมมนาวิชาการวิศวกรรมเครื่องกลแห่งประเทศไทยครั้งที่ 13
2-3 ธันวาคม 2542 โรงแรม รอยัลคลิฟบีชรีสอร์ท พัทยาใต้ ชลบุรี

การหาผลเฉลยเชิงตัวเลขของสมการเชิงอนุพันธ์ย่อย หนึ่ง และ สองมิติ ด้วยวิธีเวฟเลทคอลโลเคชัน

Numerical Solution to 1- and 2-D PDEs Using Wavelet Collocation Technique

Damrongsak Wirasaet and Pumyos Vallikul
The Waste Incineration Research Center (WIRC),
Department of Mechanical Engineering, Faculty of Engineering,
King Mongkut's Institute of Technology North Bangkok (KMITNB)
1518 Pibulsongkarm road, Bangsae, Bangkok, 10800, Thailand

บทคัดย่อ

ในงานวิจัยนี้ได้นำวิธีเวฟเลทคอลโลเคชัน ซึ่งฟังก์ชันประมาณคือฟังก์ชันออโตคอรีเลชันของดูบีชีเวฟเลทที่มีขอบเขตอัดแน่น มาใช้ในการหาผลเฉลยของสมการเชิงอนุพันธ์ย่อยชนิดหนึ่งมิติที่ไม่เป็นเชิงเส้น และชนิดสองมิติที่เป็นเชิงเส้น โดยมีเงื่อนไขขอบเขตแบบดิริชเลต์ และได้มีการศึกษาผลของจำนวนสัมประสิทธิ์ฟิลเตอร์ต่อความถูกต้องเชิงตัวเลข ปัญหาหนึ่งมิติที่เลือกใช้ในการศึกษาคือสมการเบอร์เกอร์ที่มีค่าสัมประสิทธิ์ความหนืดน้อยๆ ส่วนปัญหาในสองมิติคือสมการการนำ (สมการลาปลาซ) ได้มีการเปรียบเทียบผลลัพท์ที่คำนวณได้กับผลเฉลยที่ได้จากวิธีไฟไนท์ดิฟเฟอร์เรนซ์ และผลเฉลยวิเคราะห์ในกรณีที่สามารถหาได้ ผลเฉลยเชิงตัวเลขที่ได้แสดงให้เห็นว่าวิธีเวฟเลทคอลโลเคชันนี้ให้ผลเฉลยที่แม่นยำ และมีศักยภาพในการใช้หาผลเฉลยสำหรับปัญหาที่มีความซับซ้อนมากขึ้น

Abstract

A wavelet collocation technique, based on the auto-correlation function of Daubechies compactly supported wavelets, has been applied to solve a nonlinear 1-D and a linear 2-D PDEs of Dirichlet boundary conditions. Effects of the number of filter coefficients on numerical accuracy have been studied. The 1-D study uses the *Burgers equation* with a small viscosity as a model problem while the Laplace-conduction equation is used for the 2-D study. The numerical solutions obtained are compared with those obtained from the customary finite-difference method and the analytical solutions where possible. The numerical results indicate that the method is accurate and has the potential for solving more complicated problem.

1. Introduction

In recent years, the development of wavelet theory has attracted tremendous interest in many areas of research. One of them is the application to partial differential equations [1-5]. Wavelet-based methods have several attractions, for example, they negotiate well local sharp variations that usually cause convergence problems with the spectral methods [1, 6-8], and they are tolerant to the phase error problem when solving wave equations with finite-difference methods [6, 8]. In wavelet applications to the PDE problems, one of the most frequently used wavelets is the Daubechies compactly supported one [2-3, 9]. Most wavelet algorithms can be easily treated when the boundary conditions are of periodic type [see e.g. 1, 3, 8]. However, difficulties arise when applying such methods to solve the equation with Dirichlet boundary conditions. Wavelets are naturally bases on line so they can give rise to some instability when one uses them, without modification, in solving a Dirichlet boundary value *problem on an interval*. Recently, a wavelet collocation technique based on an auto-correlation function of Daubechies compactly supported wavelet has been proposed [4]. The auto-correlation function verifies the so-called interpolation property, and its dilations and translations generate a multiresolution analysis. These allow approximation of the solution in terms of its values at dyadic points, which verify the collocation framework of the interested problems. The boundary conditions can then simply be imposed at both ends of the approximation solution.

This paper is organized as follow: in section 2, we review the basic theory of the Daubechies compactly supported wavelet, its auto-correlation and the application of the auto-correlation function to the collocation technique. Section 3 demonstrates the solution to the Helmholtz's problem as a test problem. The effects of the number of filter coefficients on numerical accuracy are studied. In section 4, we obtain the numerical solutions to the viscous Burgers equation from the wavelet collocation method. The results are then compared with those obtained from other numerical methods. Thereafter, the algorithm for a 2-D problem is applied to the Laplace-conduction. The result agrees well with the exact and finite-difference solutions. The last section concludes the study with a discussion on future direction for research.

2. Theory

2.1 Descriptions and basic properties of the auto-correlation function of Daubechies wavelets

In this section, some properties of the auto-correlation function of Daubechies compactly supported scaling function are reviewed. To define Daubechies wavelet [10], consider the following two functions: $\phi_L(x)$ which is a solution of the scaling relation

$$\phi_L(x) = \sqrt{2}\sum_{k=0}^{L-1} h_k \phi_L(2x-k) \tag{1}$$

and the associated wavelet function defined by

$$\psi_L(x) = \sqrt{2}\sum_{k=0}^{L-1} (-1)^k h_{L-k} \phi_L(2x-k). \tag{2}$$

Where the function $\phi_L(x)$ are called the scaling function (sometimes called "father wavelet"). The filter coefficients h_k are a collection of coefficients that categorize the family wavelet basis. In order to form an orthonormal basis for $L^2(R)$, the space of square integrable functions on the real line, from the dilations and translations of the wavelet function, $2^j\psi(2^j x-k)$, and to have some degree of smooth scaling and wavelet functions, the filter coefficients must satisfy the following conditions:

Normalization: $\sum_{k=0}^{L-1} h_k = \sqrt{2}$

Orthogonality: $\sum_{k=0}^{L-1} h_k h_{k-2n} = \delta_{0,n}$

and Accuracy: $\sum_{k=0}^{L-1} (-1)^k k^l h_k = 0$,for $l = 1, 2, \ldots, M-1$.

Correspondingly, the constructed scaling function $\phi_L(x)$ and the associated wavelet function $\psi_L(x)$ have the following properties:

i) $\int \phi_L(x)dx = 1$

ii) $\int \phi_L(x)\phi_L(x-k)dx = \delta_{0,k}$

iii) $\int \phi_L(x)\psi_L(x-k)dx = 0$

iv) $\int x^l\psi(x)dx = 0$, for $l = 1, 2, \ldots, M-1$.

The vanishing moment property iv) is equivalent to the polynomial $\{1, x, x^2, \ldots, x^{M-1}\}$ written in linear combinations of scaling function, $\phi_L(x)$, and its integer translations, $\phi_L(x-k)$[11]. For the Daubechies compactly supported wavelets, the number L of the coefficients in (1) and (2) is related to the number of vanishing moment M by $L = 2M$, and the support of Daubechies scaling function, $\phi_L(x)$, is in the interval $[0, L-1]$ [10].

Let V_j and W_j, respectively, be the space spanned by the dilation and translations of the scaling function and wavelet function:

$$V_j = span\{2^{j/2}\phi_L(2^j x-k), k \in Z\}$$

and

$$W_j = span\{2^{j/2}\psi_L(2^j x-k), k \in Z\}$$

Then the following properties hold:

$$V_{j+1} = V_j \oplus W_j$$

$$\ldots \subset V_{j-1} \subset V_j \subset V_{j+1} \subset \ldots$$

$$\cap_{-\infty}^{\infty} V_j = \{0\}, \ and \ \overline{\cup_{-\infty}^{\infty} V_j} = L^2(R)$$

where $\oplus$ denotes the orthogonal direct sum. Therefore, the sequence of successive approximation spaces V_j constitutes the multiresolution of $L^2(R)$ [12].

Let $\theta(x)$ be the auto-correlation function of the Daubechies scaling function [4, 13-14],

$$\theta(x) = \int \phi_L(y)\phi_L(y-x)dy. \tag{3}$$

As a consequence of the scaling function, the auto-correlation function satisfies the following properties:

1) The support of $\theta(x)$ is in the interval $[-L+1, L-1]$.
2) By using the scaling relation, one can show that the function $\theta(x)$, also, has the scaling relation.
3) Due to the orthogonality property between the scaling function and its integer translations, the function $\theta(x)$ verifies the so-called interpolation property, that is

$$\theta(n) = \int \phi_L(y)\phi_L(y-n)dy = \delta_{0,n} .$$

4) As a consequence of iv), a polynomial of order less than L can be written as linear combinations of $\theta(x)$ and its integer translations.

The function $\theta(x)$ corresponds to the scaling function of interpolating wavelet [14-15]. Figure 1 shows the Daubechies scaling functions with $L=6$ and $L=10$ and their corresponding auto-correlation functions. By defining space $\tilde{V}_j$ as the linear span of the set $\{\theta(2^j x-k), k \in Z\}$, the sequence of $\{V_j, j \in Z\}$, also, constitute a multiresolution analysis of $L^2(R)$ and the set $\{\theta(2^j x-k), k \in Z\}$ is a Riesz's basis for $\tilde{V}_j$ [4]. The auto-correlation function $\theta(x)$, similar to $\phi_L(x)$, provides us bases on real line. In this study, the analysis is confined within the interval $[0,1]$. Modification of $\theta(x)$ to be bases on the interval $[0,1]$ having the same accuracy as that on the line can be found in [15]. That is, for $j \geq log_2(L)+1$

$$\begin{aligned}
\theta^L_{j,k}(x) &= \theta_{j,k}(x) \\
&= \theta(2^j x-k) + \sum_{n=-L+2}^{-1} a_{nk}\theta(2^j x-n), \; k=0,1,\ldots,L-1, \\
\theta_{j,k}(x) &= \theta(2^j x-k), k=L,\ldots,2^j-L \\
\theta^R_{j,k}(x) &= \theta_{j,k}(x) \\
&= \theta(2^j x-k) + \sum_{n=2^j+1}^{2^j+L-2} b_{nk}\theta(2^j x-n), \; k=2^j-L+1,\ldots,2^j
\end{aligned} \tag{4}$$

where $a_{nk} = l^L_{jk}(x_{j,n})$, and $b_{nk} = l^R_{jk}(x_{j,n})$

$$l^L_{jk}(x) = \prod_{\substack{i=0 \\ i \neq k}}^{L-1} \frac{x - x_{j,i}}{x_{j,k} - x_{j,i}}, \text{ and } l^R_{jk}(x) = \prod_{\substack{i=2^j-L+1 \\ i \neq k}}^{2^j} \frac{x - x_{j,i}}{x_{j,k} - x_{j,i}},$$

and $x_{j,k} = \dfrac{k}{2^j}$.

It is obvious from (4) that the function $\theta^L_{j,k}$ and $\theta^R_{j,k}$ still preserve the interpolation property i.e. $\theta^L_{j,k}(x_{j,n}) = \delta_{n,k}$, and $\theta^R_{j,k}(x_{j,n}) = \delta_{n,k}$, for $n, k = 0,1,\ldots,2^j$.

It is important for the application to be able to recover an arbitrary function from a discrete set of sampled values. Let $\{x_{j,k}\}_{k=0,1,\ldots,2^j}$ be a set of dyadic grid points (i.e. $x_{j,k} = k/2^j$) in interval $[0,1]$ at which function, $f(x)$, is sampled and $\{f(x_{j,k})\}_{k=0,1,\ldots,2^j}$ are the corresponding sampled values. To recover the function f, one can define the interpolation operator that maps the sampling values of the function to the space spanned by $\theta_{j,k}$, i.e. $\tilde{V}_j[0,1] = span\{\theta_{j,k}(x), k=0,\ldots,2^j\}$:

$$I_j f = \sum_{k=0}^{2^j-1} f(x_{jk})\theta_{jk}(x). \tag{5}$$

From the interpolation property of function $\theta_{j,k}$, $I_j f$ equals exactly to function f at the sampled points. The approximation property of the operator I_j is stated elsewhere [4,15].

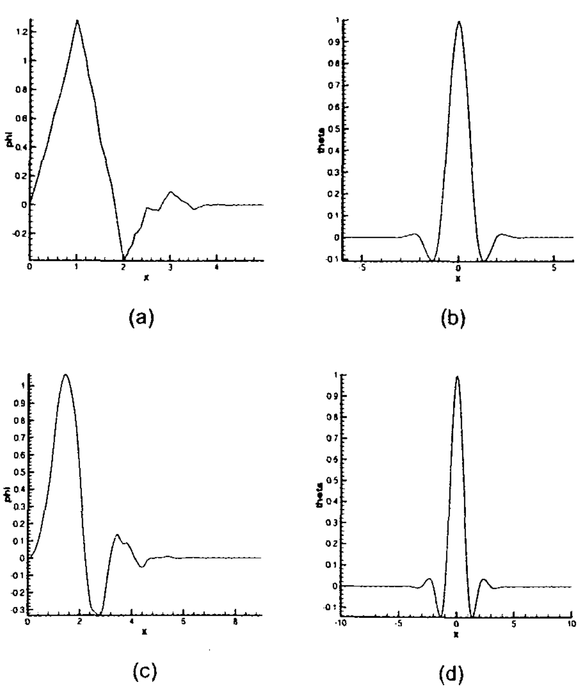

Figure 1. (a) Daubechies compactly supported scaling function with $L=6$
(b) The auto-correlation function of (a)
(c) Daubechies compactly supported scaling function with $L=10$
(d) The auto-correlation function of (c)

2.2 Wavelet collocation technique

The wavelet collocation technique used in this work was proposed by [4]. Information on other wavelet collocation techniques can be found in [16]. To implement the algorithm, consider a Dirichlet boundary value problem:

$$\begin{aligned} Au &= g \qquad , x\in(0,1) \\ u(0) &= a \\ u(1) &= b \end{aligned} \tag{6}$$

where A is the operator $-a_1(x)\frac{d^2}{dx^2}+a_2(x)\frac{d}{dx}+a_3(x)$.

The functions $a_1(x)$, $a_2(x)$, and $a_3(x)$ are bounded functions verifying $a_1>0$, $a_2>0$ and $g(x)$ is the nonhomogeneous term. We approximate the unknown solution $u(x)$ by $u_J(x)\in\tilde{V}_J[0,1]$, i.e.

$$u_J(x)=\sum_{k=0}^{2^J} u_{J,k}\theta_{j,k}(x) \tag{7}$$

where the coefficients $u_{J,k}=u_J\left(x_{J,k}=k/2^J\right)$ are unknown. The dth derivative of u_J are

$$u_J^{(d)}(x)=\sum_{k=0}^{2^J} u_{J,k}\theta_{J,k}^{(d)}(x)$$

The derivative of function $\theta(x)$ can be evaluated by

$$\theta^{(d)}(x)=(-1)^d\int\phi_L(y)\phi_L^{(d)}(y-x)dx.$$

For the integer value of x, $\theta^{(d)}(n)$ can be evaluated exactly by using the method proposed in [9]. By following the collocation approach, problem (6) reduces to

$$\begin{aligned} A_J u_J(x_{J,k}) &= g(x_{J,k}) \qquad , k=1,2,\ldots,2^J-1 \\ u_J(0) &= a \\ u_J(1) &= b \end{aligned} \tag{8}$$

where $A_J=a_1(x_{J,k})\frac{d^2}{dx^2}+a_2(x_{J,k})\frac{d}{dx}+a_3(x_{J,k})$. As seen from above, the boundary conditions are $u_{J,0}=a$ and $u_{J,2^J}=b$. After solving the system (8) for $u_{J,k}$, we then obtain the approximation solution by substitution in (7).

3. Solution to the Helmholtz's problem

In this section, we use the Helmholtz's problem as a test problem for demonstrating the effects of the number of filter coefficients, L, on numerical accuracy. The numerical results obtained from the wavelet method are compared with that from the customary finite-difference method. Consider the following boundary value problem:

$$\begin{aligned} \frac{d^2u}{dx^2}+\left(\frac{16\pi^2}{9}\right)u &= f(x) \\ u(0) &= 1 \\ u(1) &= 6.25 \end{aligned} \tag{9}$$

where

$$f(x)=-256\pi^2\sin\left(\frac{4\pi}{3}x\right)\sin\left(\frac{16\pi}{3}x\right)+ 128\pi^2\cos\left(\frac{4\pi}{3}x\right)\cos\left(\frac{16\pi}{3}x\right)$$

The exact solution to this problem is

$$u(x)=9\sin\left(\frac{4\pi}{3}x\right)\sin\left(\frac{16\pi}{3}x\right)+\cos\left(\frac{4\pi}{3}x\right) \tag{10}$$

The problem (9) is discretized into collocation framework, hence

$$\begin{aligned} \sum_{k=0}^{2^J} u_{J,k}\theta_{J,k}^{(2)}(x_{J,n})+\left(\frac{16\pi^2}{9}\right)u_{J,n} &= f_{J,n},\ n=1,2,\ldots,2^J-1 \\ u_{J,0} &= 1 \\ u_{J,2^J} &= 6.25 \end{aligned} \tag{11}$$

where $f_{J,n}=f(x_{J,n})$.

The solutions from the wavelet method ($L=10$, and $J=5$), finite-difference method, and the exact solution are compared and shown in figure 2.

To evaluate the numerical accuracy, define $\|u\|_{J,\infty}=\max_{k=1,2,\ldots,2^J-1}\left|u(x_{J,k})\right|$ and the maximum residual error by $\|u_{exact}-u_J\|_{J,\infty}$. Figure 3 shows the maximum residual errors when using the wavelet method ($L=6, 8, 10, 12,$ and 14) and the finite-difference method for various numbers of degrees of freedom (number of collocation/grid points). The figure clearly indicates that more accurate solutions are obtained when higher order wavelets are employed. Note that the reflections or flattening in the graph ($L=8$ to 14) occurs from the round off errors introduced by the computer. The slopes of the above graph, before the onset of the round-off errors, are $-(L-2)$, representing the maximum residual error decay rate, more precisely, $\|u_{exact}-u_J\|_{J,\infty}=O(2^{-J(L-2)})$. Note that, the results agree well with those obtained by the wavelet Garlerkin technique which uses the capacitance matrix method in boundary treatment [17].

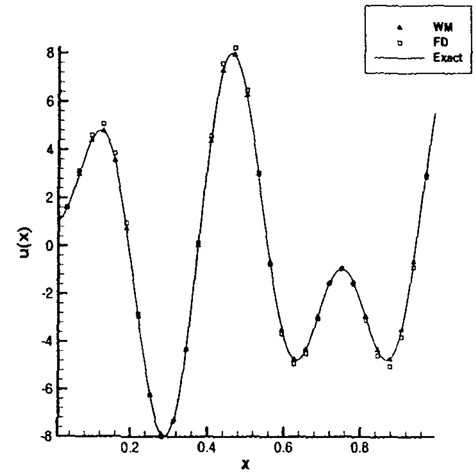

Figure 2 Solutions to the Helmholtz problem using the wavelet collocation methods ($L=10,\ J=5$), and finite-difference technique (33 grid points) compared with the exact solution.

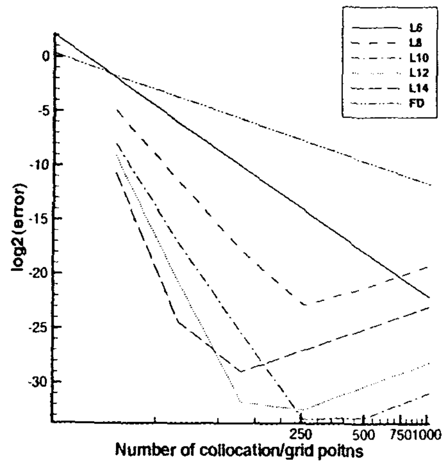

Figure 3 Maximum residual error vs. number of degrees of freedom

4. Solution to the Burgers Equation

In this section, we consider Burgers equation, which represents a first step in the hierarchy of approximations of the Navier-Stokes equation. The problem combines both the nonlinear convective and the diffusive effects. Numerical solutions to other problems that simplify Navier-Stokes equation e.g. the combined Couette-Poiseuille flow, Stokes oscillating plate, and flow in a slot with an oscillating pressure gradient have been shown in our recent work [18]. Consider the Burgers equation

$$\frac{\partial u}{\partial t}+u\frac{\partial u}{\partial x}=\nu\frac{\partial^2 u}{\partial x^2}\quad ,x\in(-1,1) \tag{12}$$

with initial and boundary conditions

$$\begin{aligned} &u(x,0)=-sin(\pi x) \\ &u(-1,t)=u(1,t)=0. \end{aligned} \tag{13}$$

In this work, the viscosity is kept small, $\nu=1/1000\pi$. We use 3rd Adam-Bashforth and Crank-Nicolson for temporal discretization of the convective and diffusive terms respectively [7] while the wavelet collocation is used in spatial discretization. Therefore, the full discretization of (12) and (13) becomes

$$\hat{u}_{J,l}=u_{J,l}^n-\frac{\Delta t}{4}\sum_{q=0}^{q=2}\alpha_q\sum_{k=0}^{2^J}(u_{J,k}^{n-q})^2\theta_{J,k}^{(1)}(x_{J,l}) \tag{14}$$

$$u_{J,l}^{n+1}-\frac{\Delta t}{8}\nu\sum_{k=0}^{2^J}u_{J,k}^{n+1}\theta_{J,k}^{(2)}(x_{J,l})=\hat{u}_{J,l}+\frac{\Delta t}{8}\nu\sum_{k=0}^{2^J}u_{J,k}^{n}\theta_{J,k}^{(2)}(x_{J,l})$$

$$u_{J,0}^n=0$$

$$u_{J,2^J}^n=0$$

$$u_{J,k}^0=-sin(\pi(2x_{J,k}-1)),\ k=1,2,\ldots,2^J-1$$

where

$$l=1,2,\ldots,2^J-1$$

$$\alpha_0=\frac{23}{12},\ \alpha_1=-\frac{4}{3},\ \alpha_2=\frac{5}{12}$$

Note that, in the numerical calculation, the domain of (12) and (13) is transformed from $x\in(-1,1)$ to $x\in(0,1)$. In solving (14), we fix the stepsize of time to be $1/1000\pi$. Figure 4 shows the solutions at different times when $J=7$ (figure 4a) and $J=10$ (figure 4b).

The numerical results are analyzed by following the method presented in [6]. The method compares the values of the maximum gradient, $\left|\frac{\partial u}{\partial x}\right|_{max}$, and its corresponding time, t_{max}, obtained from the numerical solutions with those obtained from the analytical solution. The analytical values are $\left|\frac{\partial u}{\partial x}\right|_{max}=152.0051$ and $t_{max}=1.6037\pi$. The numerical results obtained for various numbers of L and J are given in Table 1. From Table 1, for each number of L ($=6,10,14$), the maximum gradient $\left|\frac{\partial u}{\partial x}\right|_{max}$ converges to the analytical value when J is increased and vice versa. All values of t_{max} deviate slightly from the analytical value. From table 2, It has been shown that the wavelet collocation technique is competitive to the Chybyshev collocation and the Fourier Garlerkin spectral methods. However, there is an advantage in that the errors, when using wavelet collocation, do not spread over the calculated domain (see remark in Table 2). Also, the method is superior to the finite-difference when uniform grids are used.

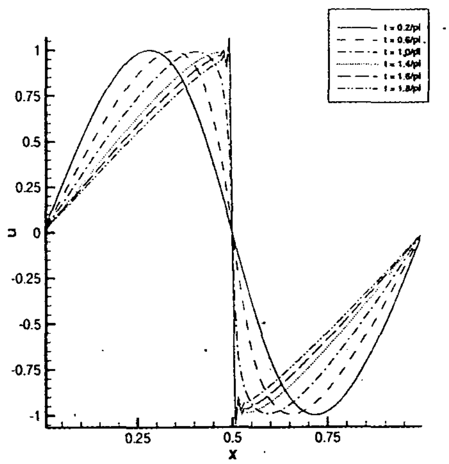

(a)

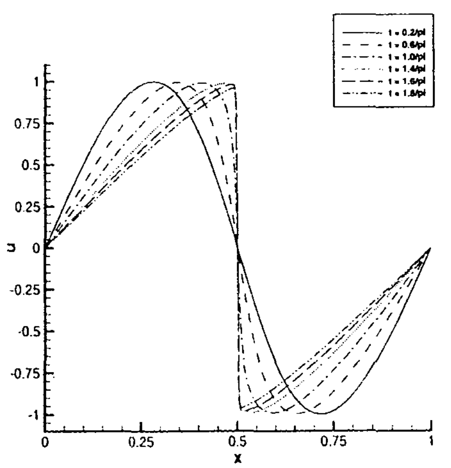

(b)

Figure 4. (a) Solution to the Burgers equation using wavelet method at $\pi t = 0.2, 0.6, 1.0, 1.4, 1.6$ and 1.8 when $L = 10$ and $J = 7$
(b) Solution to the Burgers equation using wavelet method at $\pi t = 0.2, 0.6, 1.0, 1.4, 1.6$ and 1.8 when $L = 10$ and $J = 10$

Table 1: Maximum gradient and the corresponding time for different number of filter coefficients (L) and scale (J)

L	J	Degrees of freedom	$\left\|\frac{\partial u}{\partial x}\right\|_{max}$	πt_{max}
6	7	129	80.1985	1.588
	8	257	115.1846	1.597
	9	513	140.5537	1.602
	10	1025	150.1580	1.603
	11	2049	151.8397	1.604
10	7	129	91.6758	1.590
	8	257	128.2925	1.599
	9	513	148.3872	1.603
	10	1025	151.8764	1.604
	11	2049	152.0043	1.604
14	7	129	96.7952	1.590
	8	257	132.5939	1.600
	9	513	149.8566	1.603
	10	1025	151.9731	1.604
	11	2049	152.0054	1.604
Analytic			152.0051	1.6037

Table 2: Numerical results obtained from different techniques

Methods	$\left\|\frac{\partial u}{\partial x}\right\|_{max}$	πt_{max}	Degrees of freedom	$\pi \Delta t$	remark [16]
M1[6]	151.94	1.6035	682	5×10^{-4}	NO
	142.67	1.60	682	10^{-2}	SO
	148.98	1.603	170	5×10^{-4}	SO
M2[6]	145.88	1.60	512	5×10^{-3}	SO
M3[6]	152.64	1.6033	16×4	$10^{-2}/6$	NO
M4[6]	150.14	1.63	81	10^{-2}	NO
M5[19]	66.77	1.587	129	10^{-3}	LO
	102.08	1.599	259	10^{-3}	LO
	131.34	1.602	513	10^{-3}	NO
	145.65	1.603	1025	10^{-3}	NO
Analytic	152.005	1.6037			

Note: M1 - Fourier Galerkin spectral method
M2 - Chybyshev collcation method
M3 - Uniform spectral element
M4 - Finite-difference with stretching grid
M5 - Finite-difference with uniform grid
NO - No oscillation
SO - Spread oscillation
LO – Localized oscillation

5. Solution to two-dimensional Laplace-conduction problem

The wavelet collocation technique can be generalized to a rectangular two-dimensional domain. The two-dimensional bases are constructed from tensor product of the one-dimensional function, i.e.

$$\Theta_{J,k,k'}(x,y)=\theta_{jk}(x)\theta_{j,k'}(y)\,,\,k,k'=0,1,\ldots,2^J \qquad (15)$$

where the one-dimensional function $\theta_{j,k}$ is defined by (4). The constructed bases can be used to approximate the solution of two-dimensional problems.

Consider the classical Laplace-conduction equation with Dirichlet boundary conditions:

$$\begin{aligned} &\nabla T^2=0 \;,\; x,y\in(0,1)^2 \\ &T(0,y)=0\;;\;T(1,y)=0 \\ &T(x,0)=0\;;\;T(x,1)=80 \end{aligned} \qquad (16)$$

where the exact solution to this problem is

$$T(x,y)=\frac{320}{\pi}\sum_{k=1,3,5,\ldots}^{\infty}\frac{1}{n\,sinh(n\pi)}sin(n\pi x)sinh(n\pi y)\,. \qquad (17)$$

Note that the contributions of the terms after $k=101$ are very small. The solution to the two-dimensional problem is approximated by

$$T_J(x,y)=\sum_{k=0}^{2^J}\sum_{k'=0}^{2^J}T_{J,k,k'}\Theta_{J,k,k'}(x,y)$$

where the coefficients $T_{J,k,k'}=T_J(x_{J,k},y_{J,k'})$ are unknown. The discretization of (16) in collocation framework is

$$\begin{aligned} &\sum_{k=0}^{2^J}\sum_{k'=0}^{2^J}T_{J,k,k'}\frac{\partial^2\Theta_{J,k,k'}(x_{J,n},y_{J,l})}{\partial x^2}+ \\ &\qquad\sum_{k=0}^{2^J}\sum_{k'=0}^{2^J}T_{J,k,k'}\frac{\partial^2\Theta_{J,k,k'}(x_{J,n},y_{J,l})}{\partial y^2}=0\,, \\ &T_J(0,y_{J,n})=0;T_J(1,y_{J,n})=0 \\ &T_J(x_{J,n},0)=0;T_J(x_{J,n},1)=80 \end{aligned} \qquad (18)$$

where $n,l=1,2,\ldots,2^J-1\,,\;x_{J,n},\,y_{J,n}=\dfrac{n}{2^J}$

Figures 7a and 7b show, respectively, the numerical solution of temperature contours and its absolute errors obtained from the finite-difference method. The numerical solution using wavelet technique ($L=10$, and $J=5$), and its absolute errors are plotted in figures 8a and 8b respectively. The errors of both methods are noticeable at the top-left and top-right corners. The errors, however, are confined within very small regions for the wavelet case.

6. Conclusions

The Helmholtz's problem, the viscous Burgers equation, and the two-dimensional Laplace-conduction equation with Dirichlet boundary conditions have been solved by using the wavelet collocation technique which uses the auto-correlation function as bases. The numerical results indicate that the wavelet method provides us with a high accuracy solution and the method is competitive to the well-known spectral methods and superior to the finite-difference method. Also, the algorithm can be generalized to a higher dimension in the rectangular domain. Although the one- and two-dimensional problems with Dirichlet boundary have been solved, boundary treatments using other wavelet bases are still an open problem. The approximation of the solution at multiresolution using wavelets bases would be the area of our future research.

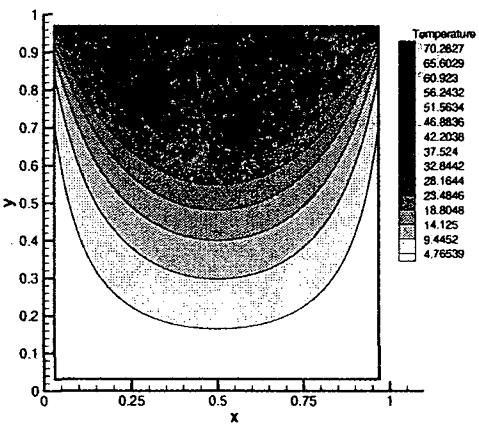

(a)

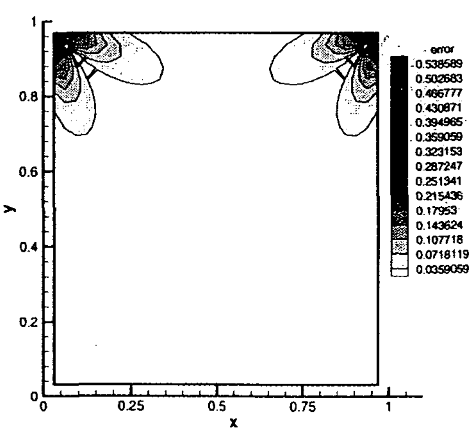

(b)

Figure 7. (a) Temperature contours of the Laplace-conduction problem using finite-difference method with 33 × 33 grid points
(b) The corresponding absolute errors of (a)

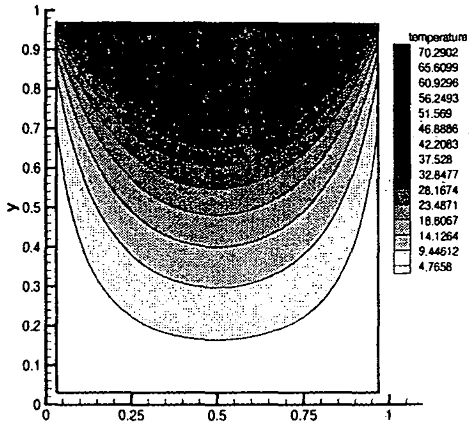

(a)

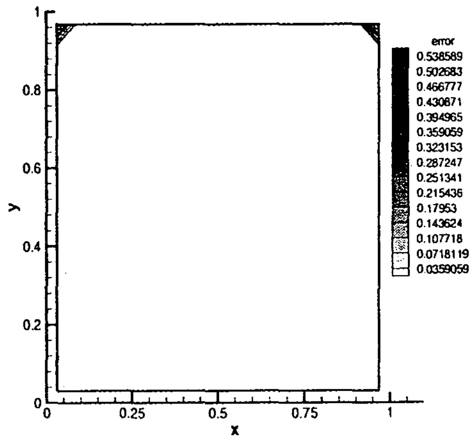

(b)

Figure 8. (a) Temperature contours of the Laplace-conduction problem using wavelet collocation technique with $L=10,\ J=5$ (33 X 33 collocation points)

(b) The corresponding absolute errors of (a)

7. Acknowledgement

We would like to thank Dr. Bundit Fungtammasn of the National Science and Technology Development Agency (NSTDA), who has assisted us prior to and all along these research efforts. Also, thanks to the High-speed Computing Laboratory at Mechanical Engineering Department, KMITNB, where this work was performed. The first author would like to thank NSTDA for the financial support through Local Graduate Scholarship (LGS).

8. References

[1] J. Liandrat, and Ph. Tchamitchian, Resolution of the 1D Regularized Burgers Equation Using a Spatial Wavelet Approximation, ICASE Report No. 90-83, 1990

[2] R. Glowinski, W. M. Lawton, M. Ravachol, and E. Tenenbaum, Wavelet Solution of Linear and Nonlinear Elliptic, Parabolic, and Hyperbolic Problems in One Space Dimension, In Proceedings of the Ninth SIAM International Conference on Computing Methods in Applied Sciences and Engineering, 1990

[3] S. Qian, and J. Weiss, Journal of Computational Physics, 106, 155-175, 1993

[4] S. Bertoluzza, and G. Naldi, Applied and Computational Harmonic Analysis, 3, 1-9, 1996

[5] L. Jameson, On the Wavelet-Optimized Finite Difference Method, ICASE Report No. 94-9, NASA, 1994

[6] C. Basdevant, M. Deville, P. Haldenwang, J. M. Lacroix, J. Ouazzani, P. Peyret, P. Orlandi, and A.T. Patera, Computer & Fluids, Vol. 14, No. 1, pp. 23-41, 1986

[7] C. Mavriplis, Computer Methods in Applied Mechanics and Engineering, 116 , pp. 77-86 , 1994

[8] D. Wirasaet, P. Vallikul, B. Fungtammasan, and P. Sukkaset, On the resolving One Dimesional PDEs with a Wavelet Collocation Technique, In Proceedings of the 12th National Mechanical Engineering Conference, Chulalongkorn University, Bangkok, Nov. 11-13, 1998

[9] G. Beylkin, SIAM J.Numer. Anal., Vol. 6., No. 6, pp. 1716-1740, 1992

[10] I. Daubechies, Ten Lecture on Wavelet, CBMS-NSF, Regional Conference Series in Applied Mathematics, 61, SIAM, 1992

[11] G. Strang, SIAM Review, Vol. 31, No. 4, pp. 614-627, 1989

[12] S. G. Mallat, Transaction of American Mathematical Society, Vol. 315, No.1, pp. 69-87, 1989

[13] N. Saito, and G. Beylkin, IEEE Transaction on Signal Processing, pp. 3584-3590, Vol. 41, No. 12, 1993

[14] G. Beylkin, and G. Saito, Wavelets, their autocorrelation functions, and multiresoltuion representation of signal, In Proceedings of SPIE-the International Society for Optical Engineering, Vol.: LB 26, P.39, 1993

[15] D. Donoho, Interpolating Wavelet Transform, Department of Statistics, Stanford University, October, 1992 (http://www-stat.standford.edu/people/faculty/donoho.html)

[16] O. V. Vasilyev ,S. M. Paolucci and M. Sen, Journal of Computational Physics, 120, 33-47, 1995

[17] K. Amaratunga, J. R. William S. Qian, and J. Weiss, International Journal for numerical Methods in Engineering, Vol. 37, 2703-2716, 1994

[18] D. Wirasaet, and P. Vallikul, Numerical Solution to 1-D Navier-Stokes Equation Using a Wavelet Collocation Technique, In Proceedings of the 3rd Annual National Symposium on Computational Science and Engineering (ANCSE), Faculty of Science, Chulalongkorn University, Bangkok, Mar. 24-29, 1999

[19] D. Wirasaet, Master Thesis (in Thai), Department of Mechanical Engineering, King Mongkut's Institute of Technology North Bangkok, in preparation